*XXIV IMEKO World Congress "Think Metrology"*
*August 26 – 29, 2024, Hamburg, Germany*

# TRANSFER STANDARD FOR THE ASSESSMENT OF SPURIOUS EMISSIONS IN DC POWER

*Guglielmo Frigo* [a, *], *Giacomo Gallus* [b]

[a]Federal Institute of Metrology METAS, Bern, Switzerland, email address: guglielmo.frigo@metas.ch
[b]University of Cagliari, Cagliari, Italy, email address: giacomo.gallus@unica.it
* Corresponding author

***Abstract*** – Low-voltage DC grids are becoming more and more popular, thanks to the possibility of integrating greener energy sources. This new power system paradigm, though, is not accounted in the current standardization framework. In particular, the power metering infrastructure is not meant to deal with signals consisting of DC components affected by AC disturbances (as the ones inherent in many renewable energy sources). This paper addresses this problem by means of an extensive measurement campaign, intended to evaluate the effect of AC disturbances on DC power meters. The obtained results point out how the limiting factor in the wide-spread of such DC grids is a lack of a proper metrology infrastructure: spanning from a proper definition of the measurand, up to a rigorous characterization of the meter influence quantities. This analysis poses the basis for a more structured approach towards a reasoned definition of performance targets for DC meters in modern power systems.

***Keywords*****:** DC meter; power measurements; harmonic distortion; calibration; measurand definition.

## 1. INTRODUCTION

In recent years, power systems are experiencing a significant transformation: the traditional paradigm based on synchronous generators is accompanied by the integration of renewable energy sources (RES) and distributed generation (DG) [1, 2]. These resources typically produce a direct current (DC) output, and their interconnection to the alternate current (AC) network relies on dedicated converters, whose power electronic circuitry switches at high frequency and produces non-negligible harmonic and inter-harmonic disturbances [3, 4, 5].

The inefficiency of such power conversion paradigm has pushed towards the development of new DC grids, expected to guarantee higher reliability and efficiency, easier control policies, and direct interface with RES, electric vehicles (EV), electronic loads (e.g. LED lighting), and energy storage systems [6, 7]. In this scenario, a distributed measurement infrastructure becomes the backbone of any monitoring and control application [8, 9].

From a metrological perspective, though, there is a lack of measurement methods for the assessment of the quality of service in DC grids. In particular, measurement campaigns carried out in real-world DC grids, e.g. the Malaga Smart City DC grid in Spain and the Lelystad Airport DC grid in the Netherlands, have demonstrated the presence of Power Quality (PQ) phenomena that may affect the metering infrastructure and cause malfunctions of appliances and utilities [10, 11].

The analysis of PQ phenomena is well established in traditional AC grids [12, 13]. The reference standard IEC 61000-4-30:2021 [14] introduces the quantities of interest and the parameters to be estimated for PQ meters. Conversely, a standard approach for PQ analysis in DC grids is not yet available. Indeed, standardisation activities in this context have mainly focused on safety rules regarding installation, wiring and fault detection. Measurement aspects, like the robustness and accuracy of metering infrastructure have not yet been properly addressed. For this reason, the IEC TC13 WG11 "Electricity metering equipment" expressed the need for developing the metrological foundations for voltage characteristics in DC grids and test waveforms for DC electricity meters, respectively [15].

In order to address these challenges, the European Metrology Programme for Innovation and Research (EMPIR) has promoted a list of research projects among the different National Metrological Institutes (NMIs) in Europe. First, the project 16ENG04 *MyRailS* considered the problem of measuring specific DCPQ events in railway supply systems and rolling stock [16]. More recently, the project 20NRM03 *DC grids* is investigating the feasibility and reliability of DC energy and power measurements in nominal and distorted conditions [17].

In this context, this paper presents a continuation of the activity presented in [18], where a transfer standard for an inter-laboratory comparison of DC power reference systems was presented. In this case, the transfer standard is used as a reference DC meter. By means of an extensive measurement campaign, the effect of AC disturbances on DC power meters is characterized, with a particular focus on the possible inconsistencies between the standard definition of measurand and the actual operating conditions in real-world installations.

The paper is structured as follows. Section 2 introduces the definition of the measurand and identifies the main challenges in real-world metering applications. In Section 3, we describe the measurement setup, focusing in particular on the measurement chain used to generate and acquire voltage and current DC signals affected by AC disturbances. Section 4 presents the measurement results and discusses how such measurement errors may be totally neglected in real-world metering installations. Finally, Section 5 draws some closing remarks and outlines the future steps of the research activity.

## 2. MEASURAND DEFINITION

The accurate measurement of DC power in nominal and distorted conditions represents a still open issue for National Metrological Institutes [19]. Indeed, such quantity lacks of a univocal definition as well as of a reference measurement method. In the IEC 62052-11:2020 [20] the DC power is introduced as the product of DC voltage and current, in turn defined as the average value of voltage and current signals.

However, neither the sampling rate nor the window length for the average computation are specified. For instance, in this regard, the EN 50470-4:2023 states the frequencies up to 10 Hz shall be considered as part of the measurement signal and the window length shall be long enough to minimize the effect of AC power components [21].

Normative efforts are currently undergoing in order to define a more rigorous and structured framework for DC power measurements. An example in this sense is the maintenance of IEC 61557-12:2021 [22] to add DC energy measurement function in line with IEC 62053-41:2021 [23].

## 3. MEASUREMENT SETUP

This section describes the setup realized at METAS for DC meter verification and calibration.

The realized setup can be divided into the part handling the generation, thus called *Generation Setup*, and the part dealing with DC power measurement, called *Measurement Setup*. The former is presented in Fig. 1 and consists of the following three stages:

- Generation Stage;
- Amplification Stage;
- Meter Stage.

The Generation Stage consists of two Keysight 33500B Function Generators responsible for generating a low-voltage DC signal with or without AC components (depending on the type of test to be performed). The two generators allow for generating an output voltage up to 10 Vpp with a wide frequency range between 1 µHz and 20 MHz with 1 µHz resolution [24]. They are also comparable with a master-slave architecture, so that in the case of the presence of AC components, signals are generated in-phase by means of a trigger coming from the device configured as master. The same trigger signal is as also used for the METAS DC meter or device under test (DUT).

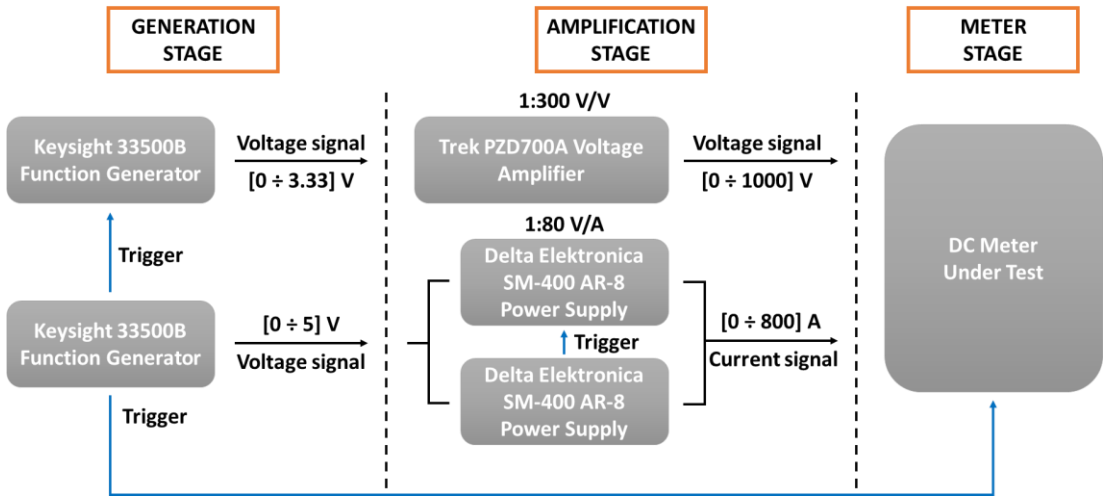


Figure 1. Block scheme of the *Generation Setup*.

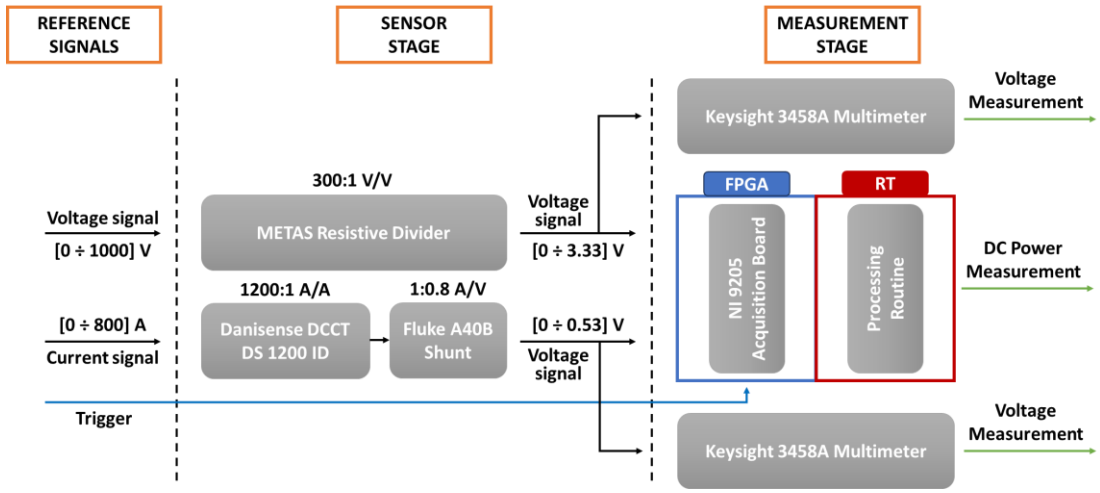


Figure 2. Block scheme of the *Measurement Setup*.

For the voltage part, the Amplification Stage consists of a Trek PZD700A wideband voltage amplifier, which allows to amplify signals up to frequencies of 200 kHz with an amplification gain of 1:300 V/V. This enables us to obtain at the end of the chain a signal up to 1000 V. The current part, on the other hand, consists of two Delta Elektronica SM-400 AR-8 Power Supplies placed in parallel in a master/slave configuration and controlled through the voltage signal from the function generator. This setup guarantees the proper amplification of signals with a spectral content of up to 300 Hz and have an amplification gain of 1:80 V/A, allowing the signal to be transduced and amplified into a current of up to 800 A (note that the devices are placed in parallel). Therefore, due to the frequency band specification of current amplifiers the generated signals may not have a frequency content higher than the 6th harmonic but this is quite realistic in a DC application where the signal bandwidth is usually less than kHz. Finally, the amplified signals are passed as input to the device under test within the Meter Stage.

The *Measurement Setup* is presented in Fig. 2 and – like the previous one – consists of three main stages:

- Reference Signal Stage;
- Sensor Stage;
- Measurement Stage.

The first stage is the result of the *Generation Setup* and thus includes the generation of the trigger signal as a time reference for the DUT as well as the voltage and current reference signals that simulate a real DC power signal.

The reference signals pass through the Sensor Stage to be properly attenuated (and transduced, in the case of the current signal), resulting in low-voltage signals compatible with the DUT analog front-end.

More precisely, the voltage signal is attenuated by means of a resistive divider made at METAS, henceforth referred to as METAS Resistive Divider, which allows by means of a purely resistive load to attenuate the voltage with a ratio of 300:1 V/V and thus obtain a maximum output signal of about 3.33 V. The current signal, on the other hand, is attenuated through a Danisense DC Current Transducer (DCCT) DS 1200 ID with a ratio of 1200:1 A/A and then transduced into a voltage signal with a Fluke A40B Shunt of 1 A, in series with the previous device, equipped with a ratio of 1:0.8 A/V. In this way, it is possible to pass from an input signal of 800 A to an output signal of about 0.53 V.

After that, within the Measurement Stage, the two low-voltage signals are measured simultaneously by the DUT and two Keysight 3458A Multimeters. The latter guarantee a measurement error of 0.15 parts per million (ppm) with respect to the read value and 0.1 ppm with respect to the measurement range, which result in 10 V and 1 V for the two signals. The multimeters thus ensure that a reference value for voltage measurements can be obtained with an accuracy in the order of µV for the case of the maximum value of the first signal and an order of magnitude less in the case of the second. Through uncertainty propagation, since this is a linear case, it is easy to estimate the uncertainty of the DC power measurement of the reference signals. Thus, by assuming zero error in the Sensor Stage for simplicity, an error on the order of hundreds of µW can be estimated. This value can be considered only as an example to understand the impact of multimeters in measuring the DC power of reference signals.

It is noteworthy that the multimeters, shunt, DCCT and METAS Divider were calibrated against the Swiss national standard ensuring traceability in measurements.

The architecture of the DC meter developed at METAS, hereafter referred to as the METAS DC Meter, is also presented in Fig. 2, which is designed to rely on hardware and software real-time (RT) and a platform equipped with Field Programmable Gate Array (FPGA) to ensure determinism of the performance. Through the FPGA, the proposed instrument is able to sample and acquire the two input voltages as soon as it receives an external trigger and send them via First In First Out (FIFO) memory to the RT software, which will handle real-time data processing. The RT software allows the data to be processed initially by correcting the systematic error, introduced by the acquisition board and the various elements of the measurement queue and estimated during the previous calibration process, using lookup tables. After that, an error compensation of the attenuators present in the Sensor Stage is carried out according to the transfer function of each device.

$$V_{\mathrm{acq}} = 0.9962 \cdot V_{\mathrm{input}} + 0.0243$$

$$I_{\mathrm{acq}} = (1 + 11\ \mathrm{ppm}) \cdot I_{\mathrm{input}} - 0.0985$$

Finally, the average of the two input signals through a window of variable size is subsequently extracted, thus estimating the DC components of the signals. By multiplying for the various attenuation ratios, the reference DC signal can be estimated, and by multiplying the two estimates with each other, the final DC power measurement is computed.

If not otherwise specified, in the following section, a window length of 0.2 s (as in AC power quality applications) or of 1 s (as a good compromise between noise reduction and update rate) is used.

The METAS DC Meter was implemented in a National Instrument (NI) CompactRIO-9068 (NI cRIO-9068), a modular system equipped with the NI Linux RT operating system and provided with ARM Cortex-A9 dual-core processor with a maximum frequency of 667 MHz and 1 GB RAM. The NI cRIO-9068 was equipped with the NI 9205 module for the acquisition of voltage signals, featuring a 16-bit Analog-to-Digital Converter (ADC) with a maximum sampling rate of 250 kHz. The board is also provided with a digital input channel that allows for triggering the acquisition with a maximum delay of 100 ns.

## 4. RESULTS AND DISCUSSION

In this Section, we present the results of a measurement campaign intended to evaluate the potential effects of AC disturbances in DC power meters. It is reasonable to expect that these effects will depend on the specific configuration adopted by the meter under test. Therefore, in the upcoming paragraphs, we attempt to characterize the contributions due to meter design parameters (i.e., window length and sampling rate) as well as disturbance entity (i.e., frequency and magnitude of the AC component).

For this analysis, we characterize the measurement errors of DC power in terms of mean (markers) and variation range (vertical bars), the latter being defined as the 95$^{\mathrm{th}}$ percentile of the error distribution. For each considered test conditions, the multimeters provide the reference value of DC voltage and current that yield the reference value of DC power. The METAS DC meter is tested for a time interval sufficient to collect 100 consecutive measurements of DC power.

First of all, it is necessary to calibrate the METAS DC meter in the presence of pure DC signals. To this end, Fig. 3 presents the DC power measurement error with a window length of 0.2 s. On the x-axis, the test points are selected to span (in a logarithmic scale) the entire range allowed by the *Generation Setup*, namely between 80 W to 800 kW. The different colours indicate different sampling rates, namely between 5 kHz to 100 kHz.

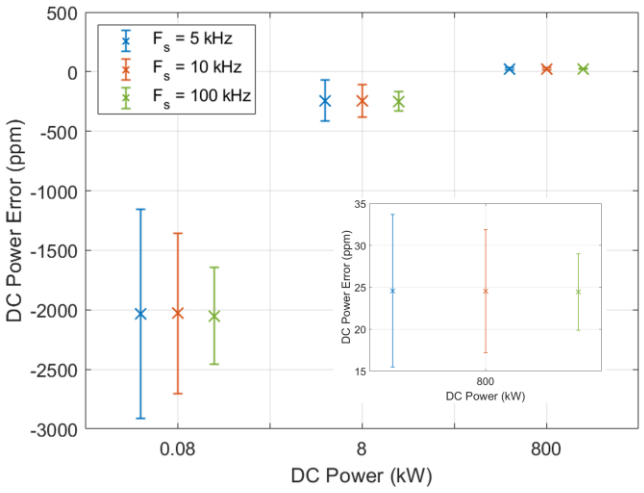


Figure 3. DC power error as function of nominal DC power with averaging interval of 0.2 s and different sampling rates.

A similar analysis is carried out for a window length of 1.0 s and is presented in Fig. 4. In both cases it is interesting to observe how both mean and variation ranges follow an exponential decay. In this regard, the inlet graphs provide a closer look at the error distribution when the DC meter input range is better exploited (i.e., at 800 kW). In general, though, it is worth noticing that a larger window length allows for reducing the error variation range at each test point, while the sampling rate has a limited impact.

By means of a non-linear fitting routine, we can identify the parameters of the exponential calibration function:

$$P_{\mathrm{err}} = a \cdot \exp(b \cdot P_{\mathrm{nom}}) + c$$

where $P_{err}$ and $P_{nom}$ represent the DC power mean error and nominal value, respectively. In this regard, Table 1 reports the values of the fitted parameters $a$, $b$, and $c$ in the two configurations.

Table 1. Exponential fit parameters as function of averaging window lenght with sampling rate equal to 10 kHz.

| $T_w$ (s) | $a$ (ppm) | $b$ (kW$^{-1}$) | $c$ (ppm) |
|---|---|---|---|
| 0.2 | -2073 | -0.11 | 24.53 |
| 1.0 | -1934 | -0.26 | 26.07 |

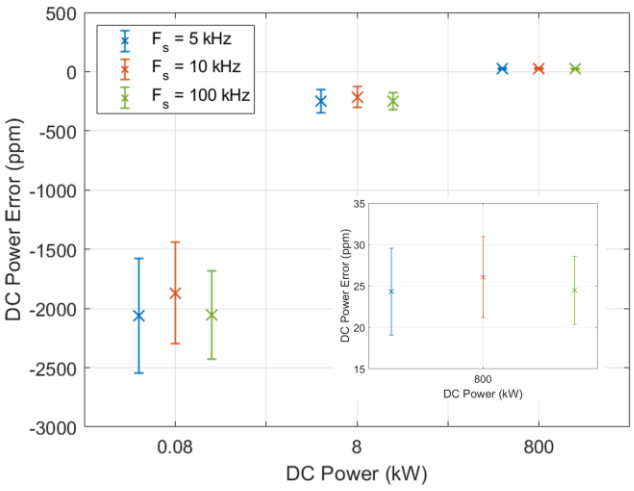


Figure 4. DC power error as function of nominal DC power with averaging window length of 1.0 s and different sampling rates.

The characterization of measurement errors in terms of mean and 95$^{th}$ percentile descend from the assumption that they are normally distributed. A proof of the validity of this assumption is given by the quantile plots in Fig. 5. For this analysis, we fix the sampling rate to 10 kHz and we consider only the test point of 8 kW. The graphical representation confirms how the measurement errors follow (reasonably) a Gaussian distribution and the use of the 95$^{th}$ percentile is a good metric of the random uncertainty contribution.

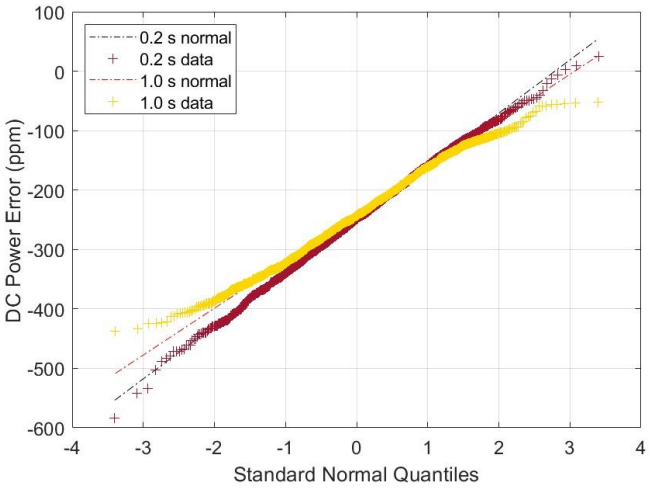


Figure 5. Quantile plot of the DC power error distributions as function of the averaging window length with a nominal value of 8 kW and a sampling rate of 10 kHz.

Once calibrated the DUT in pure DC conditions and compensated the systematic uncertainty contributions (i.e., the mean errors), we can evaluate the effect of additive AC disturbances. In the following, we consider only the test point with 8 kW since it is located at the middle of the variation range and thus represents a good trade-off between scarce and optimal resolution of the DUT. The window length is set to 1.0 s, as it is the one with lower random uncertainty.

For the sake of simplicity, the AC disturbances are here modelled as single sinusoidal tones with different frequencies and magnitudes. Given the typical bandwidth of DC meter analog front-end, we limit the frequency variation range to

300 Hz (i.e., the same as the Delta Elektronica power supply). As regards the magnitude, we define it as function of the DC voltage and current signal magnitude. In particular, we take into account two possible scenarios: low and high distortion, that corresponds to 1 % and 10 %, respectively.

The AC component is added simultaneously to both DC voltage and current signals. However, the phase displacement introduced by the two measurement chains depend on the AC component frequency. In other words, the AC components phase difference does not correspond to the ideal $\cos(\phi) = 1$ condition. Nevertheless, in this context, the AC components are influence quantities and should be discarded in the calculation of the overall active power.

Fig. 6 and Fig. 7 show the DC power error as function of the AC component frequency for the low- and high-distortion scenario, respectively. Once more, the different colours refer to different sampling rates, but this parameter has a reduced influence on the measurement results.

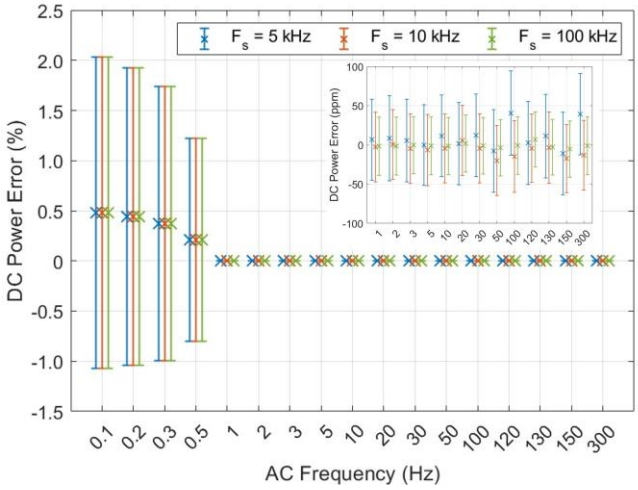


Figure 6. DC power error in the presence of a single AC interfering component with magnitude equal to 1 % of the DC one.

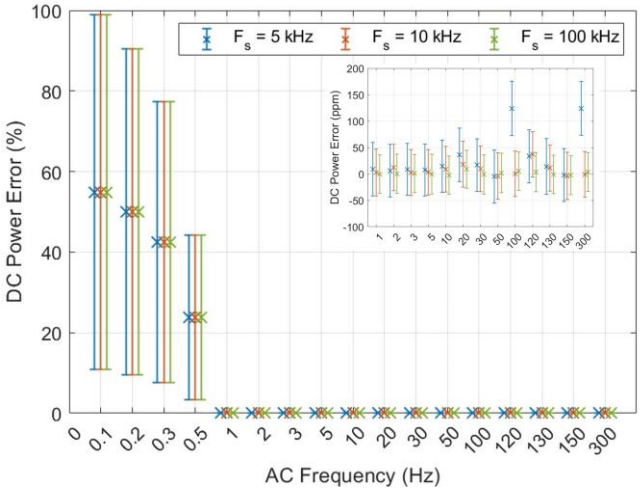


Figure 7. DC power error in the presence of a single AC interfering component with magnitude equal to 10 % of the DC one.

Given the 1.0-s window length, it is reasonable to expect that any AC component whose period is an integer divider of 1.0 s produces a nearly negligible contribution in terms of DC power error. Indeed, the average over an integer number of periods returns zero (net of measurement noise).

Conversely, the DC power error increases in a linear way as soon as the AC component frequency decreases from 1 Hz. In this case, the combined effect of AC disturbances on both voltage and current signals produces an error variation range up to 1.5 % and 45 % for low- and high-distortion scenarios.

Finally, in Fig. 8, we characterize the error dependence on the AC component magnitude. For this analysis, we fix the AC component frequency to 0.3 Hz and we vary the AC component magnitude between 1 to 10 % according to a logarithmic rule. In this case, a boxplot representation is used as it gives a straightforward intuition of how the statistical distribution changes as function of the disturbance entity.

The median as well as the extremes of the statistical distribution increases according to a quadratic law. Therefore, it is reasonable to say that the AC component effect rapidly explodes and makes the DC meter reading totally unreliable.

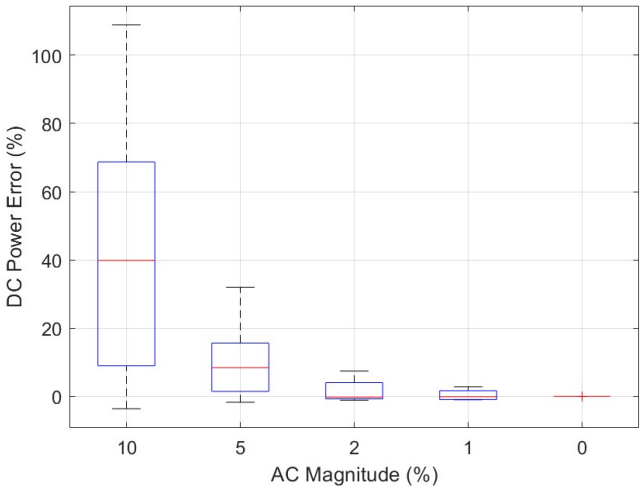


Figure 8. Boxplot of the DC power error as function of the AC component magnitude at 0.3 Hz with a sampling rate of 10 kHz.

## 5. CONCLUSIONS

In this paper, we considered the problem of DC power measurements in modern low-voltage microgrids. Due to the ever-increasing penetration of renewable energy sources and converter interconnected generation, the assumption that the power signal consists of a pure DC component is unrealistic. Unfortunately, though, the metrological infrastructure for this kind of measurements is incomplete and inconsistent with the actual conditions experienced in real-world installations.

To this end, this paper presents a measurement campaign carried out in the METAS laboratories to assess the effect of AC disturbances on a DC reference meter.

Based on the obtained results, it is clear that the main limit of the current formalization of the problem is the lack of a clear definition of the measurand. If the DC (active) power is defined as the product of mean voltage and current signals, it shall be specified which sampling rate and window length should be used for such computation. In fact, such parameters are directly related to the pass-bandwidth of the DC meter.

This analysis promises to have a significant impact on both the normalization and the certification processes. In fact, it should be noticed that the active power conveyed by the AC component should be neglected by the DC meters but has to be quantified by the system operators (either for quantifying the losses or for identifying the disturbance source).

## ACKNOWLEDGMENTS

The Authors would like to thank Dr Davide Signorino and Dr Domenico Giordano from Istituto Nazionale di Ricerca Metrologica (INRIM, Torino, Italy) for the insightful advice and guidance in the realization of the measurement setup and in the interpretation of the measurement results.

## FUNDING STATEMENT

This project (20NRM03 DC grids) has received funding from the EMPIR programme co-financed by the Participating States and from the European Union's Horizon 2020 research and innovation programme.

## REFERENCES

[1] M. Liserre, T. Sauter, J. Y. Hung, Future energy systems: Integrating renewable energy sources into the smart power grid through industrial electronics, in: IEEE Industrial Electronics Magazine, vol. 4, no. 1, pp. 18–37, 2010.

[2] A. Q. Huang, M. L. Crow, G. T. Heydt, J. P. Zheng, S. J. Dale, The future renewable electric energy delivery and management (freedom) system: The energy internet, in: Proceedings of the IEEE, vol. 99, no. 1, pp. 133–148, 2011.

[3] R. Langella, A. Testa, J. Meyer, F. Moller, R. Stiegler, S. Z. Djokic, Experimental-based evaluation of PV inverter harmonic and interharmonic distortion due to different operating conditions, in: IEEE Transactions on Instrumentation and Measurement, vol. 65, no. 10, pp. 2221–2233, 2016.

[4] M. Bollen, R. Das, S. Djokic, P. Ciufo, J. Meyer, S. Ronnberg, F. Zavodam, Power quality concerns in implementing smart distribution-grid applications, in: IEEE Transactions on Smart Grid, vol. 8, no. 1, pp. 391–399, 2017.

[5] M. Paolone, T. Gaunt, X. Guillaud, M. Liserre, S. Meliopoulos, A. Monti, T. Van Cutsem, V. Vittal, C. Vournas, Fundamentals of power systems modelling in the presence of converter-interfaced generation, in: Electric Power Systems Research, vol. 189, art. no. 106811, 2020.

[6] M. Albu, E. Kyriakides, G. Chicco, M. Popa, A. Nechifor, Online monitoring of the power transfer in a dc test grid, in: IEEE Transactions on Instrumentation and Measurement, vol. 59, no. 5, pp. 1104–1118, 2010.

[7] T. Dragicevic, X. Lu, J. C. Vasquez, J. M. Guerrero, Dc micro-grids – part II: A review of power architectures, applications, and standardization issues, in: IEEE Transactions on Power Electronics, vol. 31, no. 5, pp. 3528–3549, 2016.

[8] J. M. Guerrero, P. C. Loh, T.-L. Lee, M. Chandorkar, Advanced control architectures for intelligent microgrids – part II: Power quality, energy storage, and ac/dc microgrids, in: IEEE Transactions on Industrial Electronics, vol. 60, no. 4, pp. 1263–1270, 2013.

[9] G. Rietveld, J.-P. Braun, R. Martin, P. Wright, W. Heins, N. Ell, P. Clarkson, N. Zisky, Measurement infrastructure to support the reliable operation of smart electrical grids, in: IEEE Transactions on Instrumentation and Measurement, vol. 64, no. 6, pp. 1355–1363, 2015.

[10] M. A. Oliván, J. J. Pérez-Aragüés, J. J. Melero, A High-Frequency Digitiser System for Real-Time Analysis of DC Grids with DC and AC Power Quality Triggering, in: Applied Sciences, vol. 13, art. no. 3871, 2023.

[11] H. van den Brom, R. van Leeuwen, G. Maroulis, S. Shah, L. Mackay, Power Quality Measurement Results for a Configurable Urban Low-Voltage DC Microgrid, in: Energies, vol. 14, art. no. 4623, 2023.

[12] A. Ferrero, M. Prioli, S. Salicone, A metrological comparison between different methods for harmonic pollution metering, IEEE Transactions on Instrumentation and Measurement, vol. 61, no. 11, pp. 2972–2981, 2012.

[13] P. S. Wright, A. E. Christensen, P. N. Davis, T. Lippert, Multiple-site amplitude and phase measurements of harmonics for analysis of harmonic propagation on Bornholm island, in: IEEE Transactions on Instrumentation and Measurement, vol. 66, no. 6, pp. 1176–1183, 2017.

[14] IEC 61000-4-30:2015+AMD1:2021, Electromagnetic compatibility (EMC) Part 4-30: Testing and measurement techniques - Power quality measurement methods, International Electrotechnical Committee, 2021.

[15] CEN/CLC TC13 WG01, Testing and measurement need in research, Online [accessed on 20 Apr. 2024] https://msu.euramet.org/current_calls/pre_norm_2020/documents/cen_priority_012.pdf

[16] A. D. Femine, D. Gallo, D. Giordano, C. Landi, M. Luiso, D. Signorino, Power quality assessment in railway traction supply systems, in: IEEE Transactions on Instrumentation and Measurement, vol. 69, no. 5, pp. 2355–2366, 2020.

[17] G. Frigo, F. Costa, DC Power Metering in Low-Voltage Microgrids: Definitional and Methodological Issues, in: 2023 4th International Conference on Smart Grid Metrology (SMAGRIMET), Cavtat, Croatia, 2023, pp. 1-6.

[18] G. Frigo, M. Agustoni, Development of a Transfer Standard for DC Power Quality Reference Systems, in: 2022 IEEE 12th International Workshop on Applied Measurements for Power Systems (AMPS), Cagliari, Italy, 2022, pp. 1-6.

[19] G. Frigo, J. Braun, Measurement Setup for a DC Power Reference for Electricity Meter Calibration, in: 2022 20th International Conference on Harmonics & Quality of Power (ICHQP), Naples, Italy, 2022, pp. 1-5.

[20] IEC 62052-11:2020, Electricity metering equipment - General requirements, tests and test conditions - Part 11: Metering equipment, International Electrotechnical Committee, 2020.

[21] EN 50470-4:2023, Electricity metering equipment - Part 4: Particular requirements - Static meters for DC active energy (class indexes A, B and C), CENELEC, 2023.

[22] IEC 61557-12:2018+AMD1:2021, Electrical safety in low voltage distribution systems up to 1 000 V AC and 1 500 V DC - Equipment for testing, measuring or monitoring of protective measures - Part 12: Power metering and monitoring devices (PMD), International Electrotechnical Committee, 2021.

[23] IEC 62053-41:2021, Electricity metering equipment - Particular requirements - Part 41: Static meters for DC energy (classes 0,5 and 1), International Electrotechnical Committee, 2021.

[24] Keysight, Keysight 33500B Series Waveform Generators, Online [accessed on 20 Apr. 2024] https://www.keysight.com/us/en/assets/7018-03562/product-fact-sheets/5991-0757.pdf